Stem Cell Reports
Article

ISSCR

OPEN ACCESS

Photobiomodulation therapy for hair regeneration: A synergetic activation of β-CATENIN in hair follicle stem cells by ROS and paracrine WNTs

Huan Jin,[1,2,4] Zhengzhi Zou,[1,2,3,4] Haocai Chang,[1,2] Qi Shen,[1,2] Lingfeng Liu,[1,2] and Da Xing[1,2,*]

[1]MOE Key Laboratory of Laser Life Science & Institute of Laser Life Science, College of Biophotonics, South China Normal University, Guangzhou 510631, China

[2]Guangdong Provincial Key Laboratory of Laser Life Science, College of Biophotonics, South China Normal University, Guangzhou 510631, China

[3]Guangzhou Key Laboratory of Spectral Analysis and Functional Probes, College of Biophotonics, South China Normal University, Guangzhou 510631, China

[4]These authors contributed equally

*Correspondence: xingda@scnu.edu.cn

https://doi.org/10.1016/j.stemcr.2021.04.015

SUMMARY

Photobiomodulation therapy (PBMT) has shown encouraging results in the treatment of hair loss. However, the mechanism by which PBMT controls cell behavior to coordinate hair cycle is unclear. Here, PBMT is found to drive quiescent hair follicle stem cell (HFSC) activation and alleviate hair follicle atrophy. Mechanistically, PBMT triggers a new hair cycle by upregulating β-CATENIN expression in HFSCs. Loss of *β-Catenin (Ctnnb1)* in HFSCs blocked PBMT-induced hair regeneration. Additionally, we show PBMT-induced reactive oxygen species (ROS) activate the PI3K/AKT/GSK-3β signaling pathway to inhibit proteasome degradation of β-CATENIN in HFSCs. Furthermore, PBMT promotes the expression and secretion of WNTs in skin-derived precursors (SKPs) to further activate the β-CATENIN signal in HFSCs. By contrast, eliminating ROS or inhibiting WNT secretion attenuates the activation of HFSCs triggered by PBMT. Collectively, our work suggests that PBMT promotes hair regeneration through synergetic activation of β-CATENIN in HFSCs by ROS and paracrine WNTs by SKPs.

INTRODUCTION

Hair loss affects millions of people worldwide and usually occurs due to aging, hormonal dysfunction, mental stress, autoimmune disorder, or side effects of chemotherapy (Schneider et al., 2009). As a result, the demand for drugs to treat hair loss is increasing. Minoxidil, finasteride, and photobiomodulation therapy (PBMT) are the three hair growth promoters approved by the US Food and Drug Administration (FDA), which are commonly used in the treatment of hair loss (McElwee and Shapiro, 2012). Both minoxidil and finasteride are clinically effective drugs for the treatment of hair loss, but these two drugs may cause several side effects, such as hypertrichosis, sexual dysfunction, and fetus defect (Rogers and Avram, 2008). PBMT as a novel, convenient, drug-free, and noninvasive treatment strategy has been shown to activate hair anagen and promote hair growth. Numerous studies have shown that PBMT is an effective strategy for treating different types of hair loss without side effects in various animal models and clinical trials (Jimenez et al., 2014; Olivieri et al., 2015).

In 2007, laser comb-mediated PBMT was approved by the FDA as a safe and effective treatment for hair loss. PBMT emits monochromatic coherent collimated light. Because the coherence keeps the energy in focus and the beam is narrow, it can penetrate the scalp to the hair follicles (HFs) (Perper et al., 2017; Zarei et al., 2016). On this basis, Lee et al. (2018) designed a wearable photostimulator for hair growth in hairless mice by applying high-performance flexible red vertical light-emitting diodes (f-VLEDs). Fan et al. (2018) demonstrated that external light regulates hair follicle stem cell (HFSC) activity by stimulating the animal's eye and exerted significant hair regenerative capacity via intrinsically photosensitive retinal ganglion cells (ipRGC)/suprachiasmatic nucleus (SCN)/sympathetic neural pathway (Fan et al., 2018). These data suggested that different approaches with PBMT can promote hair regeneration; however, the precise molecular mechanisms by which PBMT promotes hair growth are not currently fully understood. Clarifying the mechanisms will explain the discrepancy of PBMT effect in different populations, and provide a theoretical basis for precise treatment.

HFSCs reside in the bulge and secondary hair germ (SHG) of HFs, orchestrated HF cyclical rounds of growth (anagen), regression (catagen), and rest (telogen) (Chen et al., 2016; Müller-Röver et al., 2001). Under numerous biological or pathological conditions, inadequate activation and proliferation inhibition of HFSCs lead to hair loss (Lei and Chuong, 2016; Paus et al., 2013). Emerging evidence suggests that HFSCs-dermal papilla (DP) interaction is essential for proper HFSCs maintenance and cell fate determination during hair regeneration (Heitman et al., 2020; Rendl et al., 2008). The WNT/β-CATENIN in HFSCs and the BMP/SMAD signaling pathway in DP mainly regulate the activation of HFSCs and the initiation of HF anagen. When the activation of WNT/β-CATENIN signaling in SHG or inhibition of BMP/SMAD signaling in DP reaches a threshold, this quiescent state is released, and activated HFSCs induce the entry of HFs into anagen (Choi et al., 2013; Genander et al., 2014; Greco et al., 2009). These results imply that

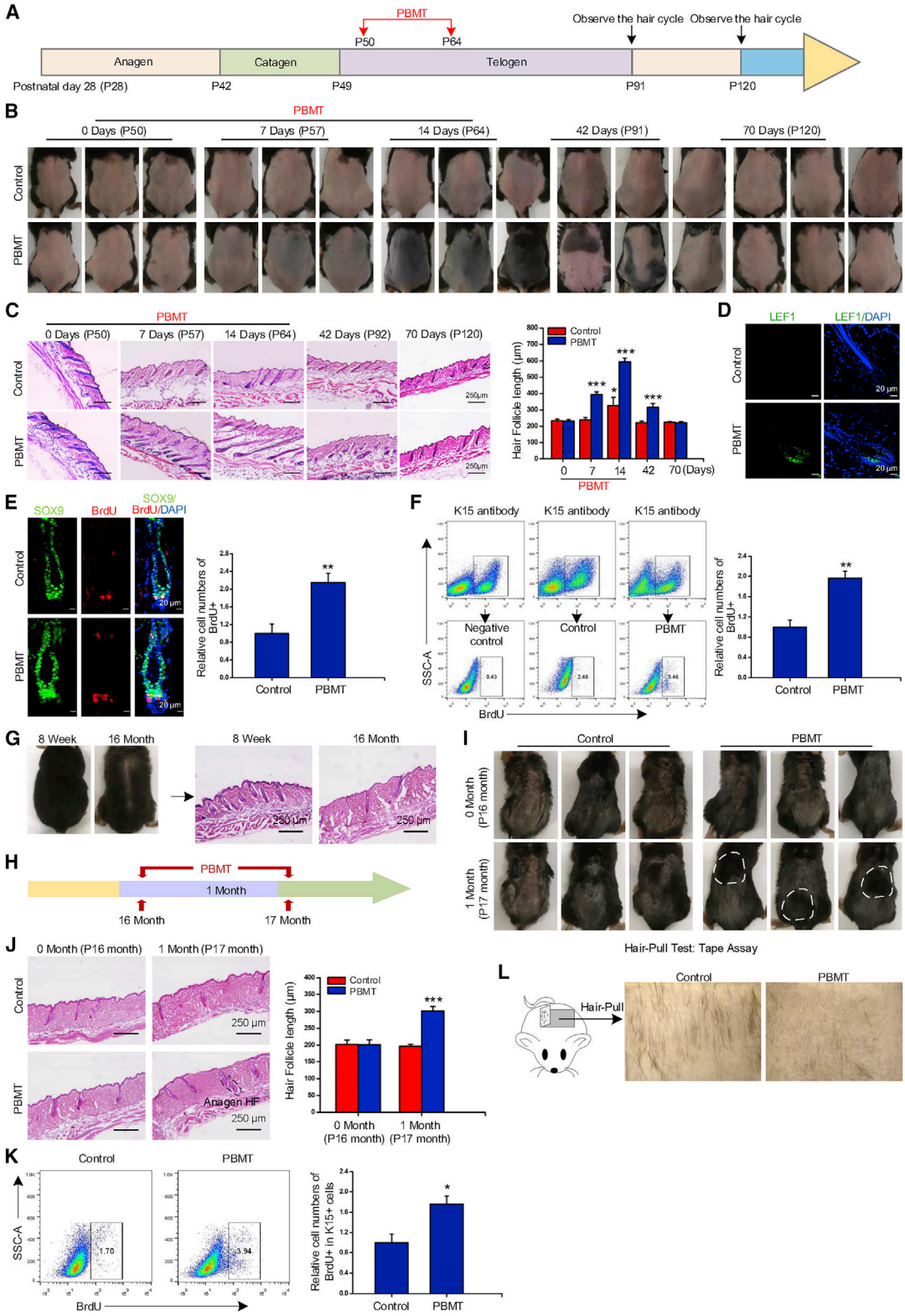

(legend on next page)

activating β-CATENIN in HFSCs may provide a powerful therapeutic strategy for hair loss. Skin-derived precursors (SKPs) are adult stem cells derived from the dermis with its niches located in the DP and dermal sheath of the HFs. Studies have shown that SKPs can regenerate DP to induce hair regeneration during HF reconstruction *in vitro* and *in vivo* (Biernaskie et al., 2009; Fernandes et al., 2004; Heitman et al., 2020). When SKPs and epidermal stem cells are transplanted into resected wounds of mice, they can induce *de novo* hair genesis, which means that SKPs have therapeutic potential in HF regeneration and bioengineering (Wang et al., 2016). However, it is unclear whether SKP-induced hair regeneration is related to the proliferation and differentiation of HFSCs.

In this study, we found that PBMT drove the activation of HFSCs and alleviated HF atrophy caused by aging. By using *Lgr5-CreER: β-Catenin$^{flox/flox}$* mice *in vivo*, and primary HFSCs and SKPs *in vitro*, we demonstrated that PBMT-stimulated reactive oxygen species (ROS) activated PI3K/AKT/GSK-3β/β-CATENIN signaling to promote HFSC proliferation. Interestingly, we also found that PBMT enhanced the HF induction ability of SKPs and increased the expression and secretion of WNTs, which activated the WNT/β-CATENIN signaling pathway in HFSCs. WNTs secreted by SKPs and ROS produced in HFSCs synergistically enhanced the GSK-3β/β-CATENIN signaling in HFSCs under PBMT conditions to enhance the potential of hair regeneration. Together, these results for the first time clarified the mechanism by which PBMT promoted hair regeneration. It provided a theoretical basis for treating hair loss by targeting skin stem cells and HFSCs in combination.

RESULTS

PBMT induces hair regeneration

In mouse, the second telogen in back skin lasts about 6 weeks starting from the seventh week of life (Müller-Röver et al., 2001). To test whether PBMT affected HF regeneration, daily PBMT (635 nm, 6.67 mW/cm^2 for 20 min, the dose reaching the epidermis was 8 J/cm^2) stimulation to the back skin was initiated on postnatal day 50 for 14 consecutive days (Figure 1A). New anagen phase activation, characterized prominent darkening of the mice back skin due to pigmentation in HFs during the anagen (Müller-Röver et al., 2001), was observed between 7 and 14 days after PBMT. On the seventh day after PBMT, the skin color of the mice in the PBMT group was changed from pink to gray, indicating that the HFs were transforming from telogen to anagen (Figure 1B). The HFs in the PBMT group were significantly longer than those in the control group on days 7 and 14 (Figure 1C). Next, we observed the morphological characteristics of HF and detected the expression of LEF1, a physiological indicator of the anagen phase of HFs (Gat et al., 1998). As shown in Figures 1D and S1A, LEF1 expression was increased in HFs and immunolocalized in SHG after PBMT.

The proliferation of HFSCs is a prerequisite for the initial anagen phase of HFs (Morris et al., 2004). Then, we investigated the proliferation ability of HFSCs induced by PBMT. BrdU (5-bromo-2'-deoxyuridine) was injected into the intraperitoneal of mouse on the third day after PBMT, and then the number of BrdU-positive cells in HFSCs was detected by flow cytometry and immunofluorescence. As shown in Figures 1E and 1F, PBMT promoted the proliferation of K15$^+$ and SOX9$^+$ HFSCs *in vivo*. All these results suggested that PBMT promoted the transformation of HFs from telogen to anagen and induced hair regeneration by activating HFSCs in mice.

HF atrophy caused by aging is a common type of hair loss (Matsumura et al., 2021). The activation of HFSCs is an effective means to alleviate aging-induced hair loss (Matsumura et al., 2016). To explore whether PBMT can alleviate hair loss caused by aging, 16-month-old mice were used in the study, as described previously (Matsumura et al., 2016) (Figures 1G and S1B). We treated the shaved old

Figure 1. PBMT induces hair regeneration

(A) Postnatal mouse hair cycle and PBMT. PBMT on the back skin every day for 14 consecutive days starting on the 50th day after birth (635 nm, 6.67 mW/cm^2, 20 min).

(B) PBMT induced telogen-anagen transition, as shown by the dorsal skin turning from pink to black, n = 12 mice.

(C) H&E images of the dorsal skin of mice at the indicated time point. n = 8 mice per group and >20 sections. *p < 0.05; ***p < 0.001.

(D) The expression of LEF1 in HFs was detected by confocal microscopy on the seventh day of PBMT, n = 8 mice per group and >60 HFs per mouse.

(E and F) The BrdU incubation experiment detected the proliferation of HFSCs by confocal (E) and flow cytometry (F), n = 8 mice.

(G and H) PBMT on the old mouse back skin every day for 1 month starting on the 16 months after birth (635 nm, 6.67 mW/cm^2, 20 min), n = 8 mice.

(I) Hair density of old mice after treatment with PBMT for 1 month, n = 8 mice.

(J) H&E images of the dorsal skin of old mice after PBMT on 1 month, n = 8 mice per group and >20 sections.

(K) Old mice after treatment with PBMT for 1 month. Flow cytometry was used to detect the proliferation of HFSCs, n = 6 mice.

(L) Tape analysis. The surgical tape was attached to the back hair of the mouse, and then it was peeled off to observe the number of hairs that fell through the tape, n = 6 mice. ANOVA was used for significance test. *p < 0.05; **p < 0.01; ***p < 0.001.

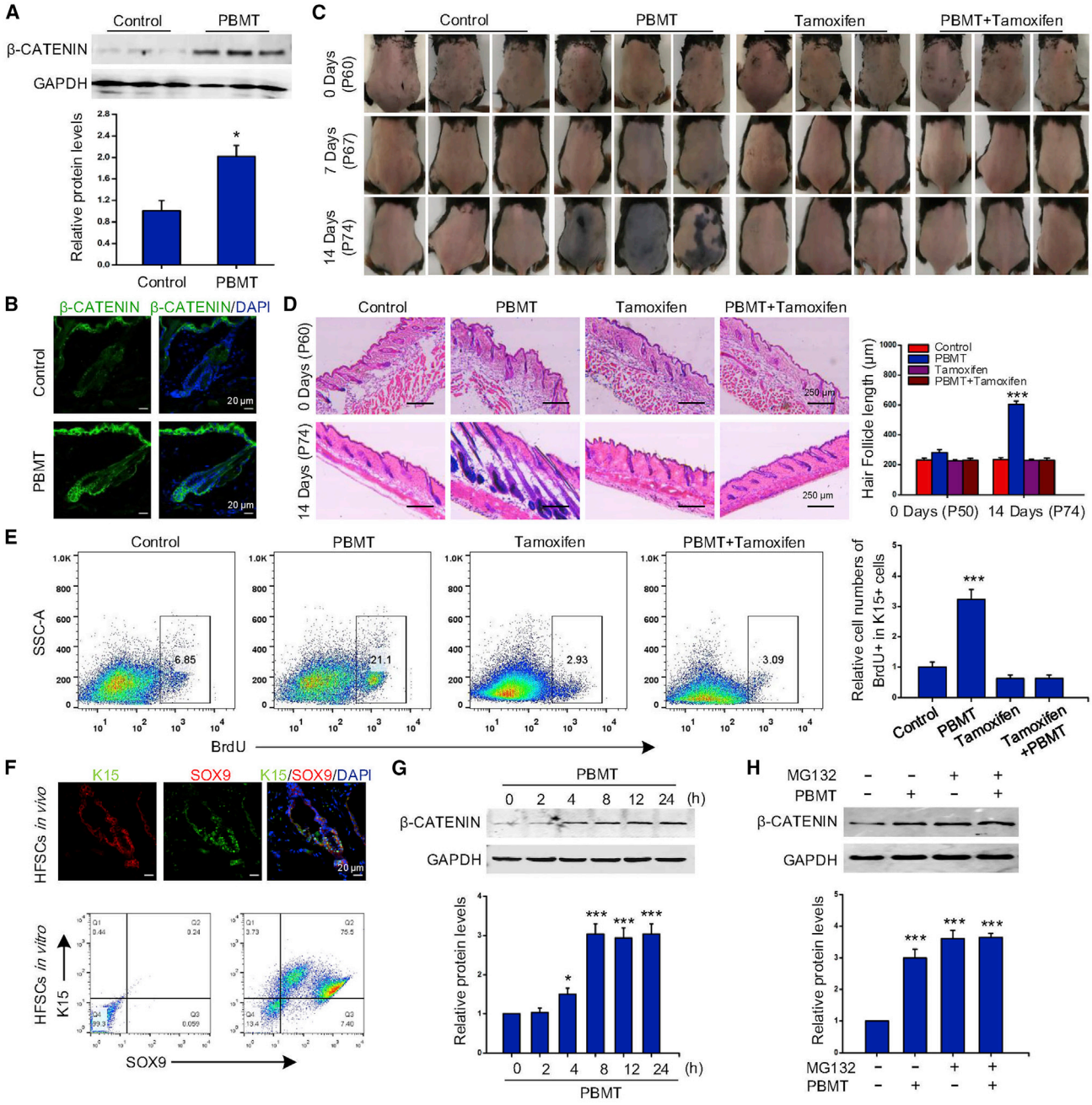

Figure 2. PBMT drives HFSC activation by inhibiting β-CATENIN degradation

(A and B) Western blot (A) and immunofluorescence (B) analysis of β-CATENIN levels after continuous PBMT treatment in mouse HF for 4 days, n = 8 mice per group and >60 HFs per mouse. ANOVA was used for significance test. *p < 0.05.

(C) Telogen-anagen transition analysis in *β-Catenin* gene knockout after PBMT, n = 6 mice.

(D) H&E images of the dorsal skin of mice after PBMT on days 14, n = 6 mice per group and >20 sections. ANOVA was used for significance test. ***p < 0.001.

(E) Flow cytometry detected the proliferation of HFSCs on the 14th day of PBMT, n = 6 mice per group and >60 HFs per mouse. ANOVA was used for significance test. ***p < 0.001.

(F) Immunofluorescence and flow cytometry were used to detect whether SOX9 and K15 in HFSCs were positive.

(legend continued on next page)

mice with PBMT for 1 month (Figure 1H). The length of the hair was greater in PBMT-treated old mice (Figure 1I). The results of HE staining showed that some HFs were in the anagen phase after PBMT treatment, and HF atrophy was alleviated by PBMT compared with the control group (Figure 1J). BrdU incorporation assays also showed that PBMT promoted the proliferation of HFSCs in old mice (Figure 1K). Next, we performed a hair-pull test by applying an adhesive surgical tape and then peeling it off from the hair coat (Lay et al., 2016). Notably, more hairs were pulled out in the control group than in the PBMT group, indicating that PBMT hairs were more difficult to pluck out than control hairs (Figure 1L). These results suggested that PBMT promoted the proliferation of HFSCs, thereby alleviating aging-induced HF atrophy.

PBMT drives HFSC activation by inhibiting β-CATENIN degradation

To explore the specific molecular mechanism by which PBMT promotes hair regeneration, we detected the expression of β-CATENIN, a key protein regulating the hair cycle in HFs. We found that the level of β-CATENIN was significantly increased by PBMT compared with the control group (Figure 2A). Immunofluorescence results showed that the expression of β-CATENIN in HF bulge and SHG was also increased (Figures 2B and S2A), suggesting that β-CATENIN might be involved in the regulation of HFSC activation induced by PBMT. Furthermore, we used *Lgr5-CreER: β-Catenin* $^{flox/flox}$ mice to test the role of β-CATENIN in PBMT-induced HFSC proliferation. According to previous reports, mice were treated with tamoxifen to induce *β-Catenin* loss in Lgr5^{+} HFSCs (*Lgr5-β-Catenin*$^{-/-}$) (Wang et al., 2017) (Figures S2B and S2C). The results in Figures 2C and 2D showed that the knockout of *β-Catenin* gene in HFSCs completely abolished PBMT-induced hair regeneration, and significantly inhibited the proliferation of HFSCs induced by PBMT (Figure 2E). These results showed that PBMT upregulated the expression of β-CATENIN in HFSCs, and knocking out the *β-Catenin* gene in HFSCs inhibited PBMT-induced hair regeneration. It suggested that PBMT induced β-CATENIN expression to drive HFSC activation *in vivo*.

To gain more insight into the specific molecular mechanism of PBMT on regulating β-CATENIN, HFSCs were isolated from newborn mice. Flow cytometry analysis showed that most of these cells were positive for SOX9 and K15, the cell markers of HFSCs (Figure 2F) (Vidal et al., 2005; Wang et al., 2017). We next tested the effects of different light doses (1.67 mW, 5 min; 3.33 mW, 5 min; 3.33 mW, 10 min; 6.67 mW, 10 min) on HFSC proliferation by Cell Counting Kit-8 (CCK-8) assay at 24 h. It was found that the light dose of 3.33 mW for 10 min exerted a greater effect on HFSC proliferation than other doses (Figure S2D). At this dose, HFSCs treated with light every 48 h for 10 days caused significantly increased colony formation (Figure S2E). These results suggested that PBMT promoted HFSC proliferation *in vitro*. By western blot assay, we showed that PBMT upregulated β-CATENIN levels in HFSCs at 8 h, consistent with the results *in vivo* (Figure 2G). β-CATENIN levels can be regulated at the transcriptional and posttranscriptional levels (Aberle et al., 2014). To explore the specific regulatory mechanisms of β-CATENIN, we first detected the mRNA levels of *β-Catenin* and its downstream genes *Lef1* and *Axin2* by qPCR. We found that *Lef1* and *Axin2* expression was increased after PBMT, but there was no significant difference in *β-Catenin* mRNA levels (Figure S2F). Next, we treated HFSCs with the proteasome inhibitor MG132 under PBMT conditions. Interestingly, MG132 enhanced β-CATENIN expression, whereas PBMT did not obviously increase β-CATENIN levels induced by MG132 (Figure 2H). These results indicated that PBMT drove HFSC activation by inhibiting β-CATENIN degradation.

PBMT stabilizes β-CATENIN by activating PI3K/AKT/GSK-3β signaling pathway

PI3K/AKT signaling pathway plays a key role in the activation of epidermal stem cell function and HF growth (Wang et al., 2017). In addition, PI3K/AKT signaling pathway is essential for HF reconstruction *in vitro* (Chen et al., 2020). The activated AKT can phosphorylate and inactivate GSK-3β at Ser9, thereby regulating the cell cycle (Zhang et al., 2019a). To evaluate whether the PI3K/AKT pathway could be affected by PBMT, we examined the expression levels of P-AKT, P-GKS-3β, and β-CATENIN in HFSCs treated with PBMT. The levels of P-AKT, P-GKS-3β, and β-CATENIN were dramatically upregulated by PBMT (Figure 3A), which was reversed by API-2 and wortmannin (specific inhibitor for AKT and PI3K respectively), suggesting that PI3K/AKT/GSK-3β signaling was essential for PBMT-induced β-CATENIN accumulation (Figure 3B). Phosphorylation of β-CATENIN on Ser552 (p-β-CAT-ser552) and dephosphorylation on Ser45 (β-CAT-ser45) stabilize β-CATENIN and enhance its transcriptional activity. HFSCs treated with PBMT significantly enhanced p-β-CAT-ser552 and β-CAT-ser45 levels, while API-2 eliminated the PBMT-induced elevation in p-β-CAT-ser552 and β-CAT-ser45 levels (Figure 3C). In

(G) The β-CATENIN protein level in mouse HFSCs was analyzed by western blot at different times after PBMT. The data represent mean ± SD, n = 3 independent replicates. *p < 0.05; ***p < 0.001.

(H) Representative western blot of HFSCs treated with PBMT for 2 h and then incubated with or without MG132 for 6 h. The data represent mean ± SD, n = 3 independent replicates. ***p < 0.001.

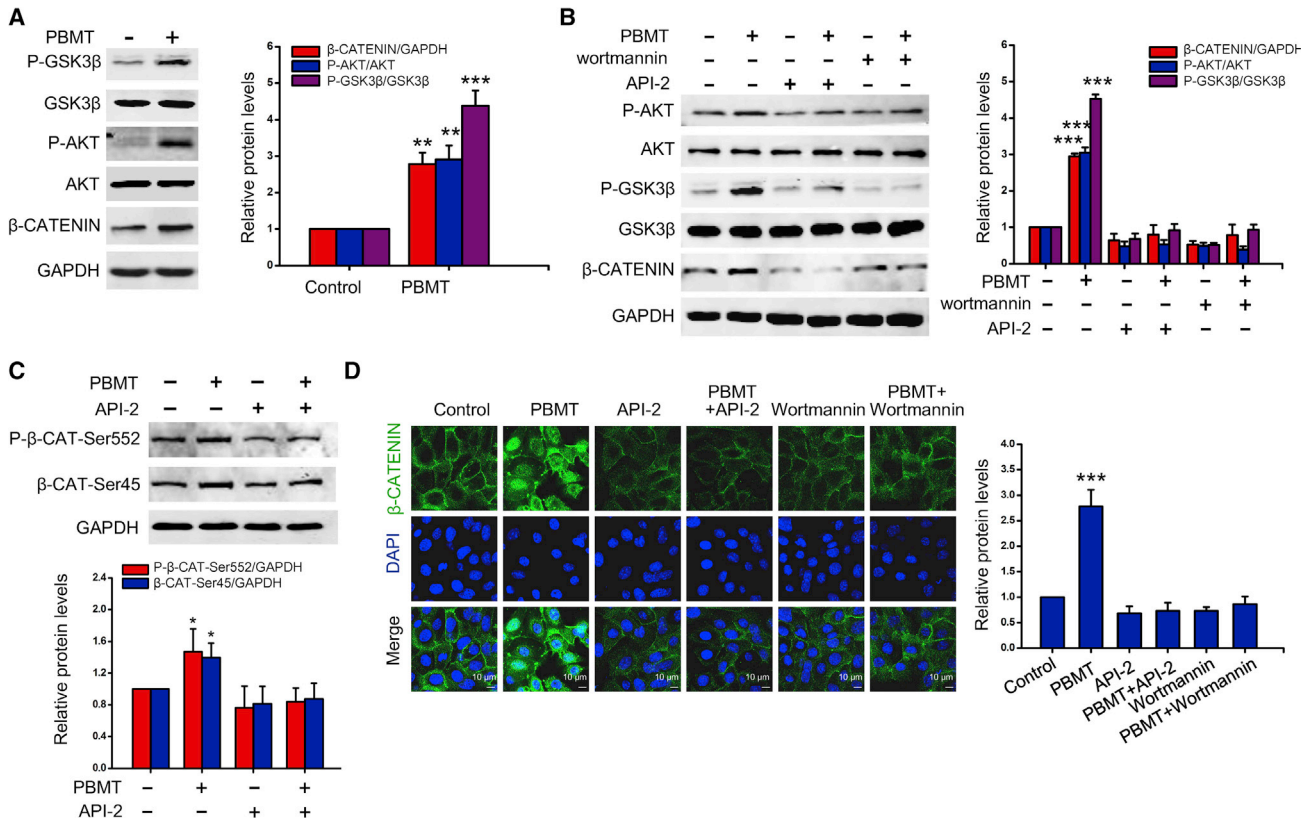

Figure 3. Activation of PI3K/AKT/GSK-3β signaling pathway by PBMT stabilizes β-CATENIN

(A) Representative western blot was performed to detect phosphorylation levels of AKT and GSK3 and β-CATENIN expression in HFSCs with or without PBMT.

(B) In the presence of API-2 and wortmannin, HFSC was stimulated with PBMT, and representative AKT and GSK3 phosphorylation levels and β-CATENIN protein levels were detected by western blot.

(C) Representative western blot assay for detecting the effect of PBMT on p-β-CATENIN (Ser552) and β-CATENIN (Ser45) proteins expression in HFSCs.

(D) Representative immunofluorescent images of β-CATENIN in HFSCs, n = 10 mice. Nuclei were stained with 4′,6-diamidino-2-phenylindole (DAPI). All the data represent mean ± SD, n = 3 independent replicates. *p < 0.05; **p < 0.01; *** p < 0.001.

addition, immunofluorescence analysis showed that PBMT enhanced the fluorescence intensity of β-CATENIN in HFSCs, and β-CATENIN level in the nucleus was also increased. However, after the HFSCs were pre-incubated with API-2 and wortmannin, PBMT markedly decreased β-CATENIN levels and prevented β-CATENIN from entering the nucleus (Figure 3D). Taken together, our results indicated that PBMT induced β-CATENIN accumulation in a PI3K/AKT/GSK-3β-dependent pathway.

PBMT activates PI3K/AKT signaling in HFSCs by inducing ROS production

ROS plays an important role in neural stem cell (NSC) and intestinal stem cell (ISC) proliferation (Le Belle et al., 2011; Myant et al., 2013). Studies have reported that light stimulation could produce low levels of ROS in normal cells (Rupel et al., 2018). We next examined whether PBMT promoted ROS generation in HFSCs. The flow cytometry and confocal microscope results showed that the dichlorofluorescein (DCF) fluorescence intensity was increased after PBMT, indicating the increase of ROS production (Figures 4A and 4B). Previous studies have demonstrated that ROS activates the PI3K/AKT signaling pathway through the reversible oxidation inactivation of the phosphatase and tensin homolog (PTEN) protein (Kwon et al., 2004). To determine whether ROS could activate PI3K/AKT signaling pathway in HFSCs. HFSCs were treated with hydrogen peroxide (H_2O_2) or PBMT. We found that both H_2O_2 and PBMT induced oxidation of PTEN protein and increase of β-CATENIN levels (Figures 4C and 4D). In addition, the phosphorylation levels of AKT and GSK-3β were also increased (Figure 4E). We next evaluated the expression of β-CATENIN and the phosphorylation of AKT and GSK-3β in the presence of antioxidant N-acetyl cysteine

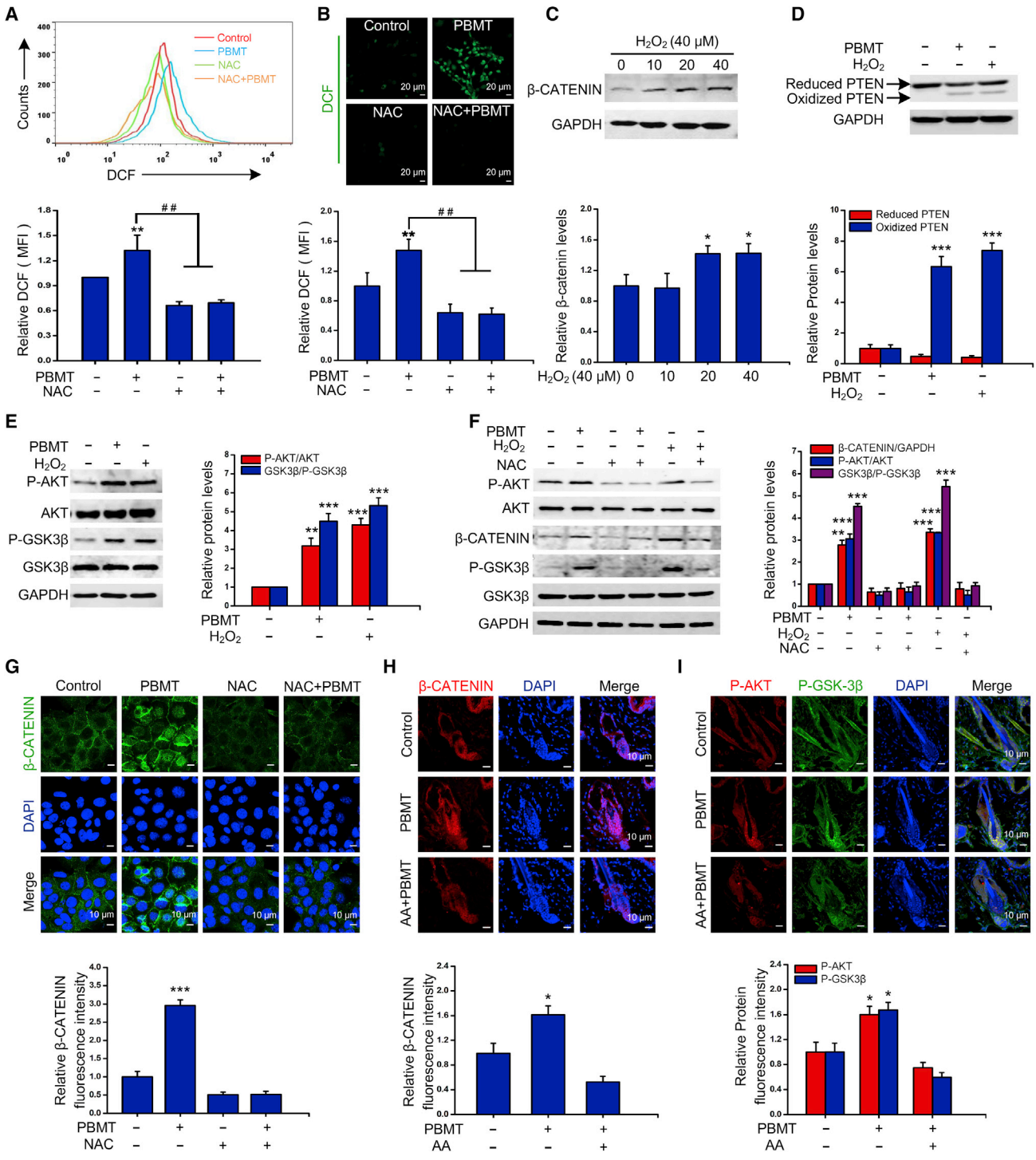

Figure 4. PBMT activates PI3K/AKT signaling in HFSCs by inducing ROS production

(A and B) HFSCs labeled with 10 μM DCF-diacetate were treated with PBMT, and the fluorescence changes were detected by flow cytometry and confocal analysis after 30 min. The data represent mean ± SD, n = 3 independent replicates. ** $p < 0.01$; ## $p < 0.01$.

(C) Western blot analysis of β-CATENIN protein levels under different concentrations of H_2O_2. The data represent mean ± SD, n = 3 independent replicates. * $p < 0.05$.

(D) Western blot analysis of oxidized and reduced PTEN levels. The data represent mean ± SD, n = 3 independent replicates. *** $p < 0.001$.

(legend continued on next page)

(NAC). As shown in Figure 4F, NAC significantly blocked PBMT-induced β-CATENIN expression and phosphorylation of AKT and GSK-3β, and eliminated the effect of exogenous H_2O_2. Furthermore, the fluorescence intensities of β-CATENIN were increased by PBMT, and β-CATENIN was obviously shown in the nucleus. After pretreatment with NAC in HFSCs, the induction and nuclear localization of β-CATENIN were completely blocked (Figure 4G).

Additionally, we pre-treated the back skin of mice with the antioxidant ascorbic acid (AA) to inhibit ROS production *in vivo* according to previous reports (Carrasco et al., 2015). We found that β-CATENIN, P-AKT, and P-GSK levels of HF bulge in mouse skin were increased by PBMT. However, AA eliminated the PBMT-induced elevation of β-CATENIN, P-AKT, and p-GSK3β levels (Figures 4H and 4I). These results suggested that PBMT-triggered ROS production was responsible for the activation of PI3K/AKT/GSK-3β signaling.

PBMT promotes HFSC proliferation by activating paracrine Wnt signals in SKPs

WNT10A, WNT10B, and WNT7B have been reported to be important secreted proteins for hair growth (Castellana et al., 2014; Kandyba and Kobielak, 2014; Reddy et al., 2001). To explore whether PBMT affected the expression of WNTs, we detected the expression of WNT10A, WNT10B, and WNT7B in skin tissue treated by PBMT. As shown in Figure 5A, PBMT significantly increased expression of WNT10A, WNT10B, and WNT7B. Importantly, we also found from immunofluorescence results that PBMT significantly promoted the expression of WNTs in the dermis (Figure 5B). Next, we separated the dermis and epithelial cell, and used flow cytometry to detect the expression of WNT10A, WNT10B, and WNT7B in the two cell populations. The results showed that PBMT promoted the expression of WNTs in the dermis cells, but there was no significant change in the epithelial cells (Figure 5C). SKPs were SOX2 and PDGFR positive when cultured *in vitro*, as shown in Figure S3A. In fibroblasts, HFSCs, and SKPs cultured *in vitro*, PBMT can significantly promote expression of WNT10A, WNT10B, and WNT7B in SKPs, but not in fibroblasts and HFSCs (Figure 5D). Immunofluorescence results also showed that PBMT promoted WNT10A, WNT10B, and WNT7B expression in SKPs (Figure 5E). Figures 5F and 5G indicate that the mRNA expression and protein secretion of WNT7B, WNT10A, and WNT10B were also increased by PBMT. To assess the effects of SKPs on HFSC proliferation under PBMT conditions, we cultured SKPs and treated them with PBMT. We found that PBMT could effectively promote the formation of large cell spheres of SKPs (Figure 5I). As shown in Figure 5H, PBMT significantly increased the expression of genes related to the ability to induce hair regeneration in SKPs, such as *Cd133*, *Alp*, *Lef1*, *Hey*, *Fgf7*, *Fgf10*, and *Sox2*. There results indicated that PBMT increased the ability of SKPs to induce HF formation. Next, we treated SKPs with PBMT, and then collected conditioned medium of SKPs (P-SKPs-CM) to culture HFSCs. Notably, P-SKPs-CM significantly increased the expression of β-CATENIN in HFSCs (Figure 5J). To further determine whether WNTs secreted by SKPs activated the classic β-CATENIN signaling in HFSCs, HFSCs were co-cultured with PBMT-treated SKPs (P-SKPs) and then were subjected to PBMT (PBMT + SKPs or PBMT + P-SKP), which further strengthened the GSK-3β/β-CATENIN signaling (Figure 5K). However, the addition of the β-CATENIN inhibitor ICG-001 significantly inhibited the proliferation of HFSCs *in vitro* (Figure 5L). Next, we treated SKPs with IWP-2, a small molecule to inhibit WNT secretion, and found that IWP-2 inhibited WNT7B, WNT10A, and WNT10B secretion (Figure S3B). Next, P-SKPs-CM was incubated with HFSCs, and we found that P-SKPs-CM increased β-CATENIN expression and GSK-3β phosphorylation levels in HFSCs, while IWP-2 pre-incubated SKPs-CM (P-IWP-2-SKPs-CM) inhibited β-CATENIN expression and GSK-3β phosphorylation (Figure S3C). Studies have shown that PBMT can regulate cell biological processes through the BMP/SMAD pathway, RAS/ERK pathway, and PI3K/AKT pathway (Feng et al., 2012; Hirata et al., 2010; Zhang et al., 2009). To explore the possible mechanisms by which PBMT promotes Wnt secretion, we used the signaling pathway inhibitors API-2 for PI3K/AKT pathway, SB525334 for BMP/SMAD pathway, and PD98059 for RAS/ERK pathway to treat SKPs. The results showed that inhibition of PI3K/AKT signal can significantly reduce the secretion of WNTs (Figure S3D), suggesting that the PIK/AKT axis was involved in the secretion process of WNTs.

(E) Representative western blot was performed to detect p-AKT, P-GKS-3β, and β-CATENIN levels under H_2O_2 and PBMT. The data represent mean ± SD, n = 3 independent replicates. ** $p < 0.01$; *** $p < 0.001$.

(F) Representative western blot analysis p-AKT, P-GKS-3β, and β-CATENIN levels of HFSCs after PBMT in the presence of NAC; the addition of exogenous H_2O_2 was used as a positive control. The data represent mean ± SD, n = 3 independent replicates. **$p < 0.01$; ***$p < 0.001$.

(G) Representative immunofluorescent images of β-CATENIN in HFSCs. Nuclei were stained with DAPI. The data represent mean ± SD, n = 3 independent replicates. ***$p < 0.001$.

(H and I) Representative immunofluorescent images of β-CATENIN (H), P-AKT, and p-GSK3β (I) in HFs, n = 8 mice per group and >60 HFs per mouse. ANOVA was used for significance test. *$p < 0.05$.

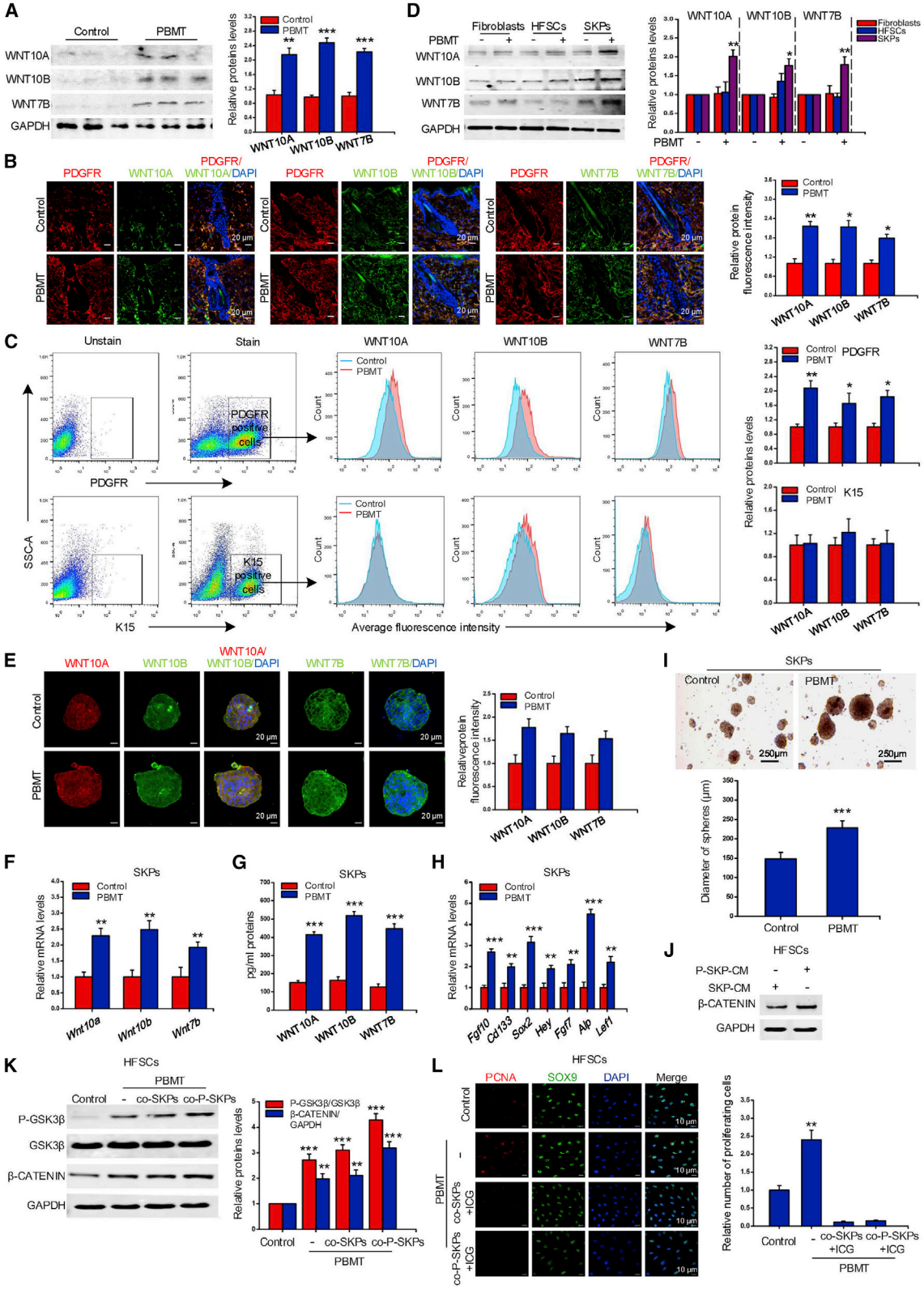

(legend on next page)

ROS and WNTs play a crucial role in PBMT-induced hair regeneration *in vivo*

We next tested whether our *in vitro* results extended to an *in vivo* HFSCs system. To this end, we tested the effects of the antioxidant AA and IWP-2 on HFSC proliferation. We had observed that PBMT promoted hair regeneration after shaving stimulation during the telogen. Importantly, the use of the AA and IWP-2 abolished the differences in HF growth rate induced by PBMT *in vivo* (Figures 6A and 6B). In addition, immunofluorescence results showed that IWP-2 seems to have a more significant inhibitory effect on WNT expression in the dermis (Figure 6C). We obtained mouse skin tissues on day 4 after PBMT, and then phosphorylated GSK-3β and β-CATENIN expression were detected in these tissues. As shown in Figure 6D, PBMT significantly increased GSK-3β phosphorylation and β-CATENIN expression. However, AA and IWP-2 eliminated the PBMT-induced elevation of GSK-3β phosphorylation and β-CATENIN levels *in vivo*. Similar results were obtained by immunofluorescence staining with antibodies against β-CATENIN and SOX9 (Figure 6E). In addition, PBMT also promoted the phosphorylation of GSK-3β and AKT in bulge and SHG cells, and these effects were suppressed by AA and IWP-2 (Figure 6F). All in all, we found that PBMT upregulated β-CATENIN expression in HFSCs. PBMT-induced ROS activated the PI3K/AKT/GSK-3β pathway to inhibit β-CATENIN degradation in HFSCs. Moreover, PBMT promoted the expression and secretion of WNTs in SKPs to further strengthen the GSK-3β/β-CATENIN signaling in HFSCs (Figure 7).

DISCUSSION

Here, our results supported previous reports that PBMT was an effective treatment for hair loss (Han et al., 2018; Jimenez et al., 2014; Olivieri et al., 2015). To our knowledge, current research provided the first evidence that PBMT promoted the proliferation of HFSCs *in vivo* and *in vitro*. PBMT as a noninvasive, nonpharmacological, and convenient approach has been widely applied in neurology, dentistry, dermatology, immunology, and regenerative medicine (Arany et al., 2014; Zhang et al., 2016, 2019b). PBMT has been approved by the FDA for the clinical treatment of hair loss (Dodd et al., 2018). Unfortunately, PBMT is only effective in a small number of patients with hair loss (Jimenez et al., 2014). In animal experiments, we found that PBMT significantly activated HFSCs, thereby promoting hair growth and preventing hair loss in mice, including aged mice. Through the study of mechanisms *in vitro* and *in vivo*, we found for the first time that PBMT induced SKPs to secrete WNTs, and then WNTs cooperated with PBMT-induced ROS to promote the proliferation of HFSCs. Our results indicated that the expression of WNTs in SKPs plays an important role in PBMT-induced hair growth. This raises a possibility that patients who failed to respond to PBMT therapy may have defects in WNT expression. Exogenous supplementation of WNTs combined with PBMT may be a potential treatment for hair loss.

Numerous studies suggested that ROS and ATP are responsible for biological functional diversity of PBMT. Studies demonstrated the biological effects induced by PBMT are caused by the absorption of photons by intracellular photoreceptors, such as cytochrome *c* oxidase in the mitochondrial respiratory chain, which leads to an electronic excited state and accelerates the electron transfer reaction. More electron transport increases mitochondrial membrane potential (MMP), which generates ATP and low levels of ROS. ROS acts as a messenger molecule, causing intracellular signal cascade effects (Khorsandi et al., 2020). Production of ROS in keratinocytes promotes the development and formation of HFs. Knockout of *Tfam*, which is required for the transcription of mitochondrial

Figure 5. PBMT promotes HFSC proliferation by activating paracrine Wnt signals in SKPs

(A) Western blot detected WNT10A, WNT10B, and WNT7B protein levels in skin tissue after PBMT, n = 8 mice.

(B) Immunofluorescence detected WNT10A, WNT10B, and WNT7B expression and localization in skin tissue, n = 8 mice per group and >60 HFs per mouse.

(C) Flow cytometry was used to detect the expression of WNT10A, WNT10B, and WNT7B in the dermis and epithelium, n = 8 mice.

(D) Western blot detected the expression of WNT10A, WNT10B, and WNT7B in fibroblasts, HFSCs, and SKPs after PBMT.

(E) The expression of WNTs in SKPs was detected by immunofluorescence, n = 10 mice.

(F) qPCR analysis of the expression of *WNTs* genes in HFSCs after PBMT.

(G) Detection of WNT10A, WNT10B, and WNT7B in SKPs culture medium by ELISA.

(H) qPCR analysis of mRNA levels of inducibility-related genes *Fgf10*, *Cd133*, *Sox2*, *Hey*, *Fgf7*, *Alp*, and *Lef1* in SKPs after PBMT.

(I) Representative spheroid image formed by SKPs with or without PBMT stimulation.

(J) Representative western blot analysis of β-CATENIN protein levels was performed in HFSCs after addition of SKPs (with or without PBMT stimulation) conditional medium.

(K) The western blot of β-CATENIN and P-GKS-3β in HFSCs that were co-cultured with SKPs as indicated: co-SKPs, co-culture with SKPs; co-P-SKPs, co-culture with PBMT-SKPs.

(L) Representative images of proliferating cell nuclear antigen (PCNA) expression in SOX9-positive HFSCs in the presence of ICG-001 (5 μM). The data represent mean ± SD, n = 3 independent replicates. *p < 0.05; **p < 0.01, ***p < 0.001.

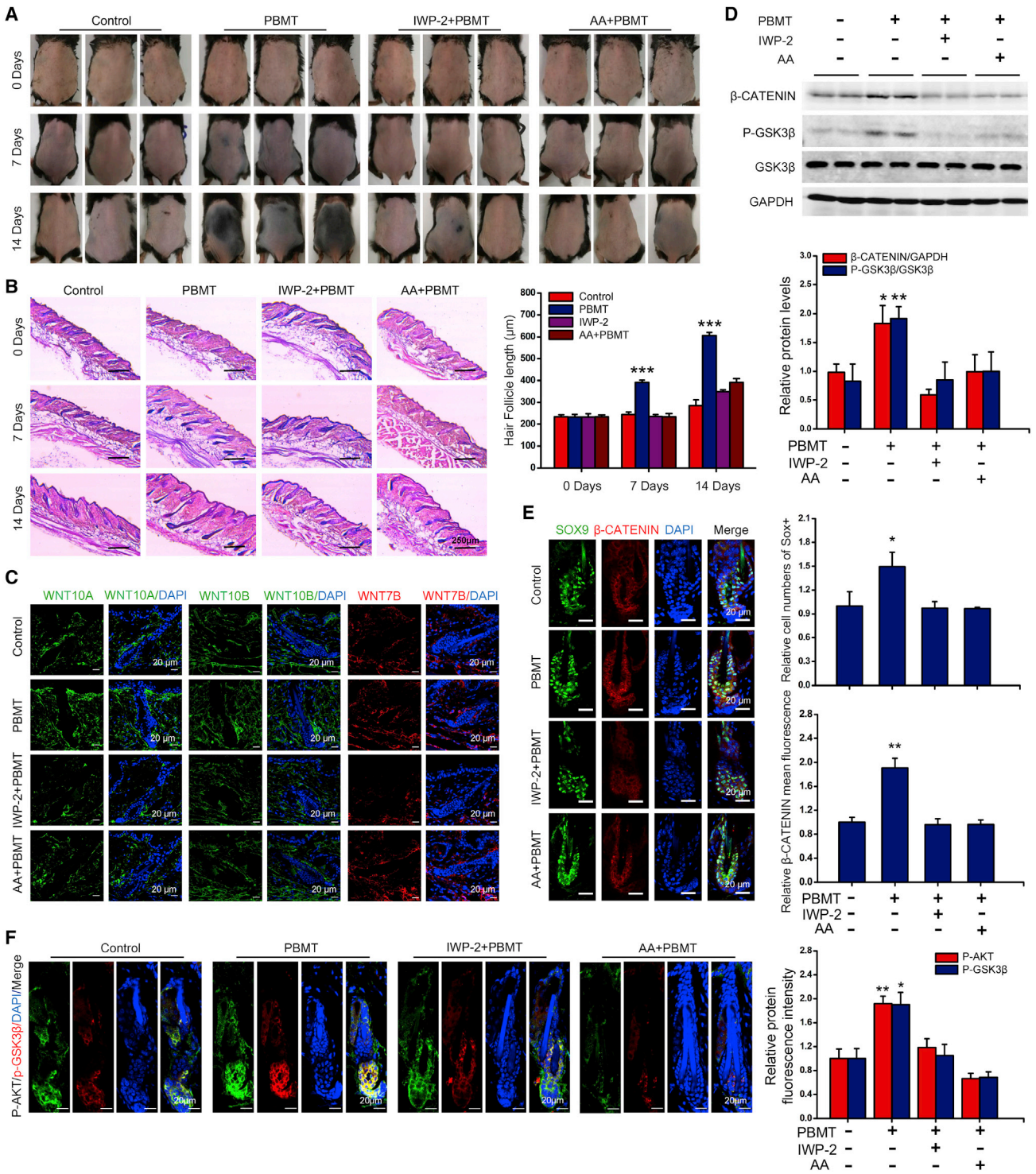

Figure 6. ROS and WNTs play a crucial role in PBMT-induced hair regeneration *in vivo*

(A and B) PBMT-induced hair growth was inhibited by AA antioxidant treatment (100 mg/mL) and IWP-2 (20 mg/kg), n = 8 mice.

(C) The expression of WNTs in mouse skin was detected by immunofluorescence after injection of IWP-2 tail vein, n = 8 mice per group and >60 HFs per mouse.

(D) Representative western blot of β-CATENIN and P-GKS-3β in skin tissues after PBMT in the presence of AA and IWP-2, n = 6 mice.

(legend continued on next page)

genes encoding electron transfer chain subunit, inhibits the production of ROS to cause HF development disorders, implying that ROS produced by mitochondria is the main factor in promoting hair growth (Hamanaka et al., 2013; Lemasters et al., 2017).

Many studies showed high levels of ROS exerted cytotoxicity, while low levels of ROS were shown to promote cell resistance to drug-induced cytotoxicity. Moreover, at low levels, ROS can also act as a messenger to activate normal cellular processes such as cell proliferation (Le Belle et al., 2011). Stem cells are generally thought to maintain low levels of ROS to execute cellular functions (Le Belle et al., 2011; Myant et al., 2013; Paul et al., 2014). Here, we directly demonstrated that PBMT-induced ROS was beneficial for the hair cycle. ROS promotes cell signal transduction and is associated with the modification of proteins by the reversible oxidation of essential cysteine residues. It has recently become clear that PTEN is crucial for stem cell maintenance. ROS can inactivate PTEN oxidation, and then regulates the proliferation and differentiation of stem cells (Hill and Wu, 2009). Deletion of the *Pten* gene in $Lgr5^+$ HFSCs significantly increases AKT signaling and shortens the second telogen phase in mice (Wang et al., 2017). Our data indicated that ROS induced by PBMT activated the PI3K/AKT signaling pathway in HFSCs. Moreover, PBMT-induced ROS promoted hair regeneration, which was similar to the phenotype observed after *Pten* gene deletion (Wang et al., 2017). These results raised a possibility that PBMT activated HFSCs to promote hair regeneration by inducing ROS to inactivate PTEN oxidation and subsequently activate PI3K/AKT pathway.

β-CATENIN controls HF morphogenesis and HFSC proliferation and differentiation in skin (Huelsken et al., 2001). Aging hair loss and androgenic alopecia are often accompanied by attenuated WNT/β-CATENIN signals, thereby prolonging the telogen phase of the HFs (GJ et al., 2017; Matsumura et al., 2016). Stable β-CATENIN expression during telogen induces HF regeneration (Deschene et al., 2014). β-CATENIN is regulated by the AXIN/APC/GSK-3β complex. GSK-3β phosphorylates β-CATENIN, causing it to degrade through the ubiquitin-proteasome pathway (Doble et al., 2007). Our data indicated that PBMT inhibited GSK-3β activity by the PI3K/AKT signaling pathway, and stabilized β-CATENIN levels in HFSCs. Knocking out *β-Catenin* gene in HFSCs inhibited PBMT-induced hair regeneration *in vivo*, suggesting that PBMT promoted hair regeneration by targeting β-CATENIN.

Adult hair follicle growth and regeneration require epithelial, dermal, and macrophage WNT ligand secretion to activate HFSCs (Myung et al., 2013). At early stages of anagen, high levels of WNT/β-CATENIN signals were observed in DP, SHG, and matrix. With the proliferation and differentiation of HFSCs, WNT/β-CATENIN signals were further increased (Choi et al., 2013). These findings suggested that WNTs play an important role in regulating hair regeneration. SKPs have been described as pluripotent dermal precursors involved in the hair cycle process (Bergeron et al., 2019). However, it is unclear how SKPs participate in the hair cycle. Our data indicated that PBMT increased the induction capacity of SKPs and promoted the expression and release of WNTs in SKPs. By co-culturing HFSCs with SKPs *in vitro*, we found that PBMT promoted WNTs secreted by SKPs to activate WNT/β-CATENIN signaling in HFSCs. Inhibition of the PI3K/AKT axis can significantly inhibit the secretion of WNTs. However, how the PI3K/AKT axis regulates the secretion process of WNTs needs further study.

This study used 7-week-old mice with HFSCs in a telogen phase and old mice with HF degeneration to explore the effect of PBMT on the hair cycle. In fact, other hair loss models, such as androgen alopecia and chemotherapy-induced alopecia, should be applied to this study to expand the application of PBMT. In addition, we have not conducted a detailed mechanism study on the expression and secretion of WNT protein. $Wntless^{fl/fl}$ mice to target loss of WNTs in $PDGFR^+$ cells should be applied to this study to explore whether PBMT can still promote hair growth after blocking WNT secretion in $PDGFR^+$ dermal cells. This detailed mechanism will be the focus of our next study. Our current study has shown that PBMT-induced ROS was involved in the activation of HFSCs. However, we did not explore whether cytochrome *c* oxidase mediated PBMT-induced ROS production in HFSCs. In the next study, we will explore the mechanisms by which PBMT induced ROS production in HFSCs.

In summary, our work revealed the mechanism by which PBMT promoted hair regeneration and demonstrated how HFSCs-SKPs interact in response to PBMT stimulation to achieve hair regeneration. The results help to clarify the functions of epithelial-dermal interactions that occur at the beginning of hair regeneration and provided new targets for the treatment of hair loss.

EXPERIMENTAL PROCEDURE

Mice

C57BL/6 female mice were purchased from Guangdong Medical Laboratory Animal Center (Guangzhou, China),

(E) Representative immunofluorescent images of β-CATENIN in $SOX9^+$ HFSCs, n = 8 mice per group and >60 HFs per mouse.
(F) Representative immunofluorescent images of P-GKS-3β and P-AKT in HFs, n = 8 mice per group and >60 HFs per mouse. ANOVA was used for significance test. *p < 0.05; **p < 0.01; ***p < 0.001.

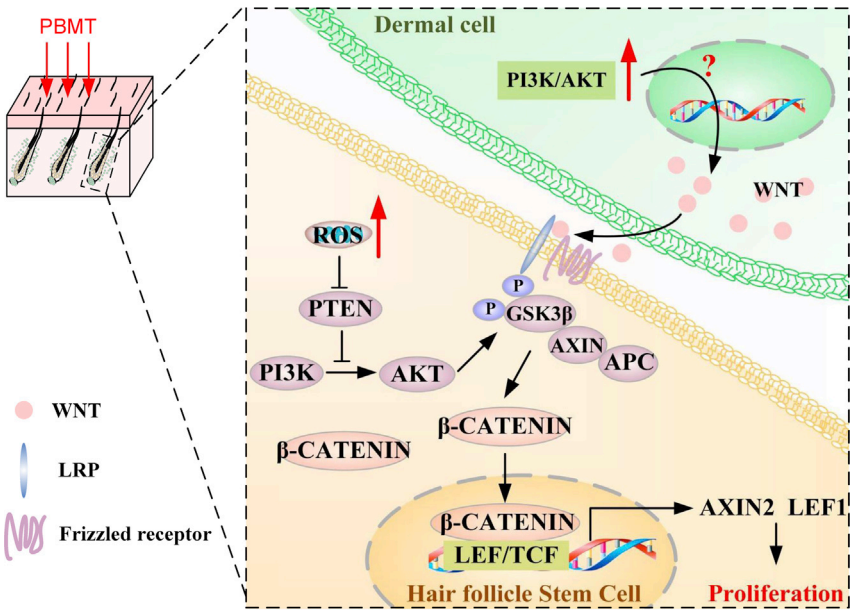

Figure 7. Model of PBMT-induced HFSC proliferation through WNT/β-CATENIN signaling

and only 7-week-old mice were used for back skin experiments. In our experiments, female C57/BL6 mice born on the same day were used and grown to 7 weeks to study the effect of PBMT on the hair cycle. At this time, the HFs of C57BL/6 mice were in the early telogen phase synchronously. Mice were kept at room temperature under a 12-h light/dark cycle with free access to food and water. *Lgr5-CreER: β-Catenin* $^{flox/flox}$ mice were provided by Dr Xusheng Wang (School of Pharmaceutical Sciences, Sun Yat-sen University). To knock out *β-Catenin* in Lgr5^{+} HFSCs, *Lgr5-Cre: β-Catenin* $^{flox/flox}$ mice aged 6–7 weeks received an intraperitoneal injection of 100 μL of tamoxifen (Sigma, T5648) in corn oil at a dose of 10 mg/mL three times (Wang et al., 2017). In the inhibition experiment of AA, we referred to the previous report (Carrasco et al., 2015). In brief, 100 mg/mL AA dissolved in 50% ethanol was used locally on the skin. After 30 min, PBMT was used on the back skin of mice (Carrasco et al., 2015). For the inhibition of Wnt secretion, as previously described, IWP2 (20 mg/kg, Abmole) was diluted in PBS, and injected intravenously every 48 h (Kling et al., 2018). All of the procedures of animal experiments were approved by the Ethics Committee of South China Normal University and performed in accordance with the Association for Assessment and Accreditation of Laboratory Animal Care guidelines (http://www.aaalac.org).

BrdU injections, and immunofluorescence and flow cytometry

After the mice were treated with PBMT, they were injected with BrdU (MCE, HY-15910) intraperitoneally at 50 mg/kg body weight. The animals were sacrificed 12 h after BrdU injection and stained with anti-BrdU antibody. The immunohistochemistry and flow cytometry procedures were performed as previously described (Pascale et al., 2020).

PBMT and HFSC co-culture with SKPs

For the *in vivo* treatment, the dorsal skin of 7-week-old female mice whose dorsal hair cycle was in the second telogen phase was carefully shaved first with an electric clipper (AUX, A5). Mice were shielded with aluminum foil head and tail to avoid light irradiation, and only the back skin was exposed. The mice were treated with the semiconductor laser (635 nm, NL-FBA-2.0-635, Light Photonics Corporation, Vancouver, WA; Laser Technology Application Research Institute, Guangzhou, China) for 14 consecutive days. After the end of PBMT, we continue to observe the mouse hair cycle in the fourth and eighth weeks. In our animal experiments, young mice were irradiated under anesthesia (2% pentobarbital, 20 mg/kg). Old mice were subjected to PBMT in a fixed state. For control, the back hair of mice was removed and the same dose of pentobarbital was injected, and they then received the same treatment without the light on. The primary cells were cultured *in vitro*, and the control group was shielded with aluminum foil and subjected to the same treatment with light. The inhibitors used in *in vitro* primary cell experiments were as follows: PD98059 (5 μM, MCE, HY-12028), SB525334 (200 nM, MCE, HY-12043), API-2 (2 μM, MCE, HY-15457), IWP-2 (5 μM, Abmole, M2237), and ICG-001 (2μM, Selleck.cn, S2662). For the *in vitro* PBMT, cells were serum-free starved for 8 h and then treated with PBMT

(10 min, 5.23 mW/cm^2). For co-culture experiments, the co-culture medium was changed (CnT-PR-CC) after the density of HFSC reached 50%–60%. After 8 h, HFSCs and SKPs were co-cultured.

Statistical analysis

All experiments were repeated three times and expressed as mean ± SD. Student's t test was used, or one-way analysis of variance (ANOVA) followed by Dunnett's post hoc tests to calculate p value, and p value <0.05 was considered a significant difference.

Data availability statement

The data used or analyzed during this study are included in this article.

SUPPLEMENTAL INFORMATION

Supplemental information can be found online at https://doi.org/10.1016/j.stemcr.2021.04.015.

AUTHOR CONTRIBUTIONS

D.X., Z.Z., and H. J. developed the concept. H.J. and Z.Z. designed and performed experiments, analyzed and interpreted data, and co-wrote the manuscript. H.C., Q.S., and L.F. contributed to experiments and helped with data interpretation. All authors edited and reviewed the final manuscript.

CONFLICT OF INTERESTS

There are no competing financial interests.

ACKNOWLEDGMENTS

This work was supported by the National Natural Science Foundation of China (81772803, 81972479, 61627827, and 62005085), Science and Technology Program of Guangzhou (2019050001), Scientific and Technological Planning Project of Guangzhou City (201904010038), Natural Science Foundation of Guangdong province (2019A1515011100 and 2021A1515012576). We thank Dr. Xusheng Wang (School of Pharmaceutical Science-Shenzhen, Sun Yat-sen University) for kindly providing *β-Catenin$^{flox/flox}$* and *Lgr5-GFP-Cre-ERT2 (Lgr5-Cre)* mice.

Received: August 30, 2020
Revised: April 21, 2021
Accepted: April 22, 2021
Published: May 20, 2021

REFERENCES

Aberle, H., Bauer, A., Stappert, J., Kispert, A., and Kemler, R. (2014). β-catenin is a target for the ubiquitin–proteasome pathway. EMBO J. *16*, 3797–3804.

Arany, P.R., Cho, A., Hunt, T.D., Sidhu, G., Shin, K., Hahm, E., Huang, G.X., Weaver, J., Chen, A.C.-H., and Padwa, B.L. (2014). Photoactivation of endogenous latent transforming growth factor–β1 directs dental stem cell differentiation for regeneration. Sci Transl Med *6*, 238–269.

Bergeron, L., Busuttil, V., and Botto, J.M. (2019). Multipotentiality of skin-derived precursors. Application to the regeneration of skin and other tissues. Int. J. Cosmet. Sci. *42*, 5–15.

Biernaskie, J., Paris, M., Morozova, O., Fagan, B., Marra, M., Pevny, L., and Miller, F. (2009). SKPs derive from hair follicle precursors and exhibit properties of adult dermal stem cells. Cell Stem Cell *5*, 610–623.

Carrasco, E., Calvo, M., Blázquez-Castro, A., Vecchio, D., Zamarrón, A., de Almeida, I., Stockert, J., Hamblin, M., Juarranz, Á., and Espada, J. (2015). Photoactivation of ROS production in situ transiently activates cell proliferation in mouse skin and in the hair follicle stem cell niche promoting hair growth and wound healing. J. Invest. Dermatol. *135*, 2611–2622.

Castellana, D., Paus, R., and Perez-Moreno, M. (2014). Macrophages contribute to the cyclic activation of adult hair follicle stem cells. PLoS Biol. *12*, 1002002.

Chen, C., Plikus, M., Tang, P., Widelitz, R., and Chuong, C. (2016). The modulatable stem cell niche: tissue interactions during hair and feather follicle regeneration. J. Mol. Biol. *428*, 1423–1440.

Chen, Y., Fan, Z., Wang, X., Mo, M., Zeng, S., Xu, R., Wang, X., and Wu, Y. (2020). PI3K/AKT signaling pathway is essential for de novo hair follicle regeneration. Stem Cell Res. Ther. *11*, 144.

Choi, Y.S., Zhang, Y., Xu, M., Yang, Y., Ito, M., Peng, T., Cui, Z., Nagy, A., Hadjantonakis, A.K., Lang, R.A., et al. (2013). Distinct functions for WNT/beta-catenin in hair follicle stem cell proliferation and survival and interfollicular epidermal homeostasis. Cell Stem Cell *13*, 720–733.

Deschene, E.R., Myung, P., Rompolas, P., Zito, G., Sun, T.Y., Taketo, M.M., Saotome, I., and Greco, V. (2014). β-Catenin activation regulates tissue growth non–cell autonomously in the hair stem cell niche. Science *343*, 1353–1356.

Doble, B.W., Patel, S., Wood, G.A., Kockeritz, L.K., and Woodgett, J.R. (2007). Functional redundancy of GSK-3α and GSK-3β in WNT/β-catenin signaling shown by using an allelic series of embryonic stem cell lines. Dev. Cell *12*, 957–971.

Dodd, E., Winter, M., Hordinsky, M., Sadick, N., and Farah, R. (2018). Photobiomodulation therapy for androgenetic alopecia: a clinician's guide to home-use devices cleared by the Federal Drug Administration. J. Cosmet. Laser Ther. *20*, 159–167.

Fan, S.M.Y., Chang, Y.T., Chen, C.L., Wang, W.H., Pan, M.K., Chen, W.P., Huang, W.Y., Xu, Z., Huang, H.-E., and Chen, T. (2018). External light activates hair follicle stem cells through eyes via an ipRGC–SCN–sympathetic neural pathway. Proc. Natl. Acad. Sci. U S A *115*, 6880–6889.

Feng, J., Zhang, Y., and Xing, D. (2012). Low-power laser irradiation (LPLI) promotes VEGF expression and vascular endothelial cell proliferation through the activation of ERK/Sp1 pathway. Cell. Signal. *24*, 1116–1125.

Fernandes, K., McKenzie, I., Mill, P., Smith, K., Akhavan, M., Barnabé-Heider, F., Biernaskie, J., Junek, A., Kobayashi, N., Toma, J., et al. (2004). A dermal niche for multipotent adult skin-derived precursor cells. Nat. Cell Biol. *6*, 1082–1093.

Gat, U., DasGupta, R., Degenstein, L., and Fuchs, E. (1998). De novo hair follicle morphogenesis and hair tumors in mice expressing a truncated β-catenin in skin. Cell *95*, 605–614.

Genander, M., Cook, P., Ramsköld, D., Keyes, B., Mertz, A., Sandberg, R., and Fuchs, E. (2014). BMP signaling and its pSMAD1/5 target genes differentially regulate hair follicle stem cell lineages. Cell Stem Cell *15*, 619–633.

GJ, L., JM, C., ML, C., AG, K., and ME, B. (2017). Androgens modify Wnt agonists/antagonists expression balance in dermal papilla cells preventing hair follicle stem cell differentiation in androgenetic alopecia. Mol. Cell. Endocrinol. *439*, 26–34.

Greco, V., Chen, T., Rendl, M., Schober, M., Pasolli, H., Stokes, N., Dela Cruz-Racelis, J., and Fuchs, E. (2009). A two-step mechanism for stem cell activation during hair regeneration. Cell Stem Cell *4*, 155–169.

Hamanaka, R., Glasauer, A., Hoover, P., Yang, S., Blatt, H., Mullen, A., Getsios, S., Gottardi, C., DeBerardinis, R., Lavker, R., et al. (2013). Mitochondrial reactive oxygen species promote epidermal differentiation and hair follicle development. Sci. Signal. *6*, 8.

Han, L., Liu, B., Chen, X., Chen, H., Deng, W., Yang, C., Ji, B., and Wan, M. (2018). Activation of WNT/β-catenin signaling is involved in hair growth-promoting effect of 655-nm red light and LED in in vitro culture model. Lasers Med. Sci. *33*, 637–645.

Heitman, N., Sennett, R., Mok, K., Saxena, N., Srivastava, D., Martino, P., Grisanti, L., Wang, Z., Ma'ayan, A., Rompolas, P., et al. (2020). Dermal sheath contraction powers stem cell niche relocation during hair cycle regression. Science *367*, 161–166.

Hill, R., and Wu, H. (2009). PTEN, stem cells, and cancer stem cells. J. Biol. Chem. *284*, 11755–11759.

Hirata, S., Kitamura, C., Fukushima, H., Nakamichi, I., Abiko, Y., Terashita, M., and Jimi, E. (2010). Low-level laser irradiation enhances BMP-induced osteoblast differentiation by stimulating the BMP/Smad signaling pathway. J. Cell. Biochem. *111*, 1445–1452.

Huelsken, J., Vogel, R., Erdmann, B., Cotsarelis, G., and Birchmeier, W. (2001). β-catenin controls hair follicle morphogenesis and stem cell differentiation in the skin. Cell *105*, 533–545.

Jimenez, J.J., Wikramanayake, T.C., Bergfeld, W., Hordinsky, M., Hickman, J.G., Hamblin, M.R., and Schachner, L.A. (2014). Efficacy and safety of a low-level laser device in the treatment of male and female pattern hair loss: a multicenter, randomized, sham device-controlled, double-blind study. Am. J. Clin. Dermatol. *15*, 115–127.

Kandyba, E., and Kobielak, K. (2014). WNT7B is an important intrinsic regulator of hair follicle stem cell homeostasis and hair follicle cycling. Stem Cells (Dayton, Ohio) *32*, 886–901.

Khorsandi, K., Hosseinzadeh, R., Abrahamse, H., and Fekrazad, R. (2020). Biological responses of stem cells to photobiomodulation therapy. Curr. Stem Cell Res. Ther. *15*, 400–413.

Kling, J., Jordan, M., Pitt, L., Meiners, J., Thanh-Tran, T., Tran, L., Nguyen, T., Mittal, D., Villani, R., Steptoe, R., et al. (2018). Temporal regulation of natural killer T cell interferon gamma responses by β-catenin-dependent and -independent wnt signaling. Front Immunol *9*, 483–494.

Kwon, J., Lee, S., Yang, K., Ahn, Y., Kim, Y., Stadtman, E., and Rhee, S. (2004). Reversible oxidation and inactivation of the tumor suppressor PTEN in cells stimulated with peptide growth factors. Proc. Natl. Acad. Sci. U S A *101*, 16419–16424.

Lay, K., Kume, T., and Fuchs, E. (2016). FOXC1 maintains the hair follicle stem cell niche and governs stem cell quiescence to preserve long-term tissue-regenerating potential. Proc. Natl. Acad. Sci. U S A *113*, 1506–1515.

Le Belle, J.E., Orozco, N.M., Paucar, A.A., Saxe, J.P., Mottahedeh, J., Pyle, A.D., Wu, H., and Kornblum, H.I. (2011). Proliferative neural stem cells have high endogenous ROS levels that regulate self-renewal and neurogenesis in a PI3K/AKT-dependant manner. Cell Stem Cell *8*, 59–71.

Lee, H.E., Lee, S.H., Jeong, M., Shin, J.H., Ahn, Y., Kim, D., Oh, S.H., Yun, S.H., and Lee, K.J. (2018). Trichogenic photostimulation using monolithic flexible vertical AlGaInP light-emitting diodes. ACS Nano *12*, 9587–9595.

Lei, M., and Chuong, C. (2016). STEM CELLS. Aging, alopecia, and stem cells. Science *351*, 559–560.

Lemasters, J., Ramshesh, V., Lovelace, G., Lim, J., Wright, G., Harland, D., and Dawson, T. (2017). Compartmentation of mitochondrial and oxidative metabolism in growing hair follicles: a ring of fire. J. Invest. Dermatol. *137*, 1434–1444.

Matsumura, H., Liu, N., Nanba, D., Ichinose, S., and Nishimura, E.K. (2021). Distinct types of stem cell divisions determine organ regeneration and aging in hair follicles. Nat. Aging *1*, 190–204.

Matsumura, H., Mohri, Y., Binh, N., Morinaga, H., Fukuda, M., Ito, M., Kurata, S., Hoeijmakers, J., and Nishimura, E. (2016). Hair follicle aging is driven by transepidermal elimination of stem cells via COL17A1 proteolysis. Science *351*, 4395.

McElwee, K.J., and Shapiro, J. (2012). Promising therapies for treating and/or preventing androgenic alopecia. Skin Ther. Lett. *17*, 1–4.

Morris, R.J., Liu, Y., Marles, L., Yang, Z., Trempus, C., Li, S., Lin, J.S., Sawicki, J.A., and Cotsarelis, G. (2004). Capturing and profiling adult hair follicle stem cells. Nat. Biotechnol. *22*, 411.

Müller-Röver, S., Handjiski, B., van der Veen, C., Eichmüller, S., Foitzik, K., McKay, I., Stenn, K., and Paus, R. (2001). A comprehensive guide for the accurate classification of murine hair follicles in distinct hair cycle stages. J. Invest. Dermatol. *117*, 3–15.

Myant, K.B., Cammareri, P., McGhee, E.J., Ridgway, R.A., Huels, D.J., Cordero, J.B., Schwitalla, S., Kalna, G., Ogg, E.-L., and Athineos, D. (2013). ROS production and NF-κB activation triggered by RAC1 facilitate WNT-driven intestinal stem cell proliferation and colorectal cancer initiation. Cell Stem Cell *12*, 761–773.

Myung, P., Takeo, M., Ito, M., and Atit, R. (2013). Epithelial Wnt ligand secretion is required for adult hair follicle growth and regeneration. J. Invest. Dermatol. *133*, 31–41.

Olivieri, L., Cavina, D., Radicchi, G., Miragliotta, V., and Abramo, F. (2015). Efficacy of low-level laser therapy on hair regrowth in dogs with noninflammatory alopecia: a pilot study. Vet. Dermatol. *26*, 35–39.

Pascale, E., Beclin, C., Fiorenzano, A., Andolfi, G., Erni, A., De Falco, S., Minchiotti, G., Cremer, H., and Fico, A. (2020). Long non-coding RNA T-UCstem1 controls progenitor proliferation

and neurogenesis in the postnatal mouse olfactory bulb through interaction with miR-9. Stem Cell Rep. *15*, 836–844.

Paul, M.K., Bisht, B., Darmawan, D.O., Chiou, R., Ha, V.L., Wallace, W.D., Chon, A.T., Hegab, A.E., Grogan, T., and Elashoff, D.A. (2014). Dynamic changes in intracellular ROS levels regulate airway basal stem cell homeostasis through Nrf2-dependent Notch signaling. Cell Stem Cell *15*, 199–214.

Paus, R., Haslam, I., Sharov, A., and Botchkarev, V. (2013). Pathobiology of chemotherapy-induced hair loss. Lancet Oncol. *14*, 50–59.

Perper, M., Aldahan, A., Fayne, R., Emerson, C., and Nouri, K. (2017). Efficacy of fractional lasers in treating alopecia: a literature review. Lasers Med. Sci. *32*, 1919–1925.

Reddy, S., Andl, T., Bagasra, A., Lu, M., Epstein, D., Morrisey, E., and Millar, S. (2001). Characterization of Wnt gene expression in developing and postnatal hair follicles and identification of Wnt5a as a target of Sonic hedgehog in hair follicle morphogenesis. Mech. Dev. *107*, 69–82.

Rendl, M., Polak, L., and Fuchs, E. (2008). BMP signaling in dermal papilla cells is required for their hair follicle-inductive properties. Genes Dev. *22*, 543–557.

Rogers, N.E., and Avram, M.R. (2008). Medical treatments for male and female pattern hair loss. J. Am. Acad. Dermatol. *59*, 547–566.

Rupel, K., Zupin, L., Colliva, A., Kamada, A., Poropat, A., Ottaviani, G., Gobbo, M., Fanfoni, L., Gratton, R., Santoro, M., et al. (2018). In vitro photobiomodulation at multiple wavelengths differentially modulates oxidative stress and. Oxid. Med. Cell. longev. *2018*, 6510159.

Schneider, M.R., Schmidt-Ullrich, R., and Paus, R. (2009). The hair follicle as a dynamic miniorgan. Curr. Biol. *19*, 132–142.

Vidal, V., Chaboissier, M., Lützkendorf, S., Cotsarelis, G., Mill, P., Hui, C., Ortonne, N., Ortonne, J., and Schedl, A. (2005). SOX9 is essential for outer root sheath differentiation and the formation of the hair stem cell compartment. Curr. Biol. *15*, 1340–1351.

Wang, X., Chen, H., Tian, R., Zhang, Y., Drutskaya, M.S., Wang, C., Ge, J., Fan, Z., Kong, D., and Wang, X. (2017). Macrophages induce AKT/β-catenin-dependent $Lgr5^+$ stem cell activation and hair follicle regeneration through TNF. Nat. Commun. *8*, 14091.

Wang, X., Wang, X., Liu, J., Cai, T., Guo, L., Wang, S., Wang, J., Cao, Y., Ge, J., and Jiang, Y. (2016). Hair follicle and sebaceous gland de novo regeneration with cultured epidermal stem cells and skin-derived precursors. Stem Cell Transl. Med. *5*, 1695–1706.

Zarei, M., Wikramanayake, T., Falto-Aizpurua, L., Schachner, L., and Jimenez, J. (2016). Low level laser therapy and hair regrowth: an evidence-based review. Lasers Med. Sci. *31*, 363–371.

Zhang, H., Su, Y., Wang, J., Gao, Y., Yang, F., Li, G., and Shi, Q. (2019a). Ginsenoside Rb1 promotes the growth of mink hair follicle via PI3K/AKT/GSK-3β signaling pathway. Life Sci. *229*, 210–218.

Zhang, L., Xing, D., Gao, X., and Wu, S. (2009). Low-power laser irradiation promotes cell proliferation by activating PI3K/AKT pathway. J. Cell. Physiol. *219*, 553–562.

Zhang, Q., Dong, T., Li, P., and Wu, M.X. (2016). Noninvasive low-level laser therapy for thrombocytopenia. Sci. Transl. Med. *8*, 349.

Zhang, Z., Shen, Q., Wu, X., Zhang, D., and Xing, D. (2019b). Activation of PKA/SIRT1 signaling pathway by photobiomodulation therapy reduces Aβ levels in Alzheimer's disease models. Aging Cell *19*, 13054.